Environmental Science & Technology

pubs.acs.org/est

Article

The Role of Hydrates, Competing Chemical Constituents, and Surface Composition on $ClNO_2$ Formation

Haley M. Royer, Dhruv Mitroo, Sarah M. Hayes, Savannah M. Haas, Kerri A. Pratt, Patricia L. Blackwelder, Thomas E. Gill, and Cassandra J. Gaston*

Cite This: https://dx.doi.org/10.1021/acs.est.0c06067

Read Online

ACCESS | Metrics & More | Article Recommendations | Supporting Information

ABSTRACT: Atomic chlorine ($Cl^•$) affects air quality and atmospheric oxidizing capacity. Nitryl chloride ($ClNO_2$) – a common $Cl^•$ source–forms when chloride-containing aerosols react with dinitrogen pentoxide (N_2O_5). A recent study showed that saline lakebed (playa) dust is an inland source of particulate chloride (Cl^-) that generates high $ClNO_2$. However, the underlying physiochemical factors responsible for observed yields are poorly understood. To elucidate these controlling factors, we utilized single particle and bulk techniques to determine the chemical composition and mineralogy of playa sediment and dust samples from the southwest United States. Single particle analysis shows trace highly hygroscopic magnesium and calcium Cl-containing minerals are present and likely facilitate $ClNO_2$ formation at low humidity. Single particle and mineralogical analysis detected playa sediment organic matter that hinders N_2O_5 uptake as well as 10 Å-clay minerals (e.g., Illite) that compete with water and chloride for N_2O_5. Finally, we show that the composition of the aerosol surface, rather than the bulk, is critical in $ClNO_2$ formation. These findings underscore the importance of mixing state, competing reactions, and surface chemistry on N_2O_5 uptake and $ClNO_2$ yield for playa dusts and, likely, other aerosol systems. Therefore, consideration of particle surface composition is necessary to improve $ClNO_2$ and air quality modeling.

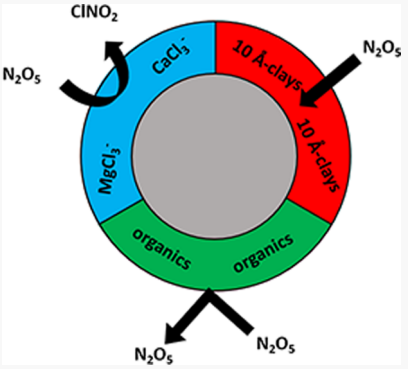

KEYWORDS: *aerosol, halogen, air quality, heterogeneous reaction, dinitrogen pentoxide, nitryl chloride, mineral dust, hygroscopicity*

1. INTRODUCTION

Halogen radicals, such as atomic chlorine ($Cl^•$), are highly reactive oxidants that can affect both regional air quality and Earth's climate.[1] For example, $Cl^•$ can react with volatile organic compounds (VOCs) in the atmosphere to produce secondary organic aerosols (SOA),[2] which comprise a majority of the fine aerosol loading.[3,4] Reactions between $Cl^•$ and VOCs can also produce tropospheric ozone (O_3),[5,6] which is a greenhouse gas and criteria air pollutant. From a climate perspective, $Cl^•$ can also lower the lifetime of methane (a potent greenhouse gas).[7,8]

A common formation pathway for $Cl^•$ begins with the nighttime heterogeneous reaction between gaseous dinitrogen pentoxide (N_2O_5), a NO_x reservoir compound, and deliquesced chloride-containing (Cl-containing) particles.[5,9] N_2O_5 reacts with deliquesced particles with an efficiency referred to as its reactive uptake coefficient (γ_{N2O5}), defined as the probability that an N_2O_5 molecule will undergo an irreversible reaction when it collides with a particle. In the absence of particulate chloride (Cl^-), N_2O_5 will undergo a hydrolysis reaction producing two nitric acid (HNO_3) molecules (R1).[10,11] In the presence of deliquesced Cl^- ($Cl^-_{(aq)}$), N_2O_5 will react with $Cl^-_{(aq)}$ to form nitrate (NO_3^-) and a nitryl chloride ($ClNO_2$) molecule (R2).[5,9,12,13] The amount of $ClNO_2$ produced per amount of N_2O_5 reacted from R2 is referred to as $ClNO_2$ yield (ϕ_{ClNO2}).

$$N_2O_5(g) + H_2O(aq) \rightarrow 2HNO_3(aq) \quad \text{(R1)}$$

$$N_2O_5(g) + Cl^-(aq) \rightarrow ClNO_2(g) + NO_3^-(aq) \quad \text{(R2)}$$

Previous research has shown that the rate of R2 is 400–800 times larger than R1,[5,12,14] suggesting that R2 is favored, even when $Cl^-_{(aq)}$ concentrations are small. $ClNO_2$ then accumulates in the gas phase during the night and photolyzes into a $Cl^•$ and a NO_2 radical at sunrise (R3).[15]

$$ClNO_2 + h\nu \rightarrow Cl^• + NO_2 \quad \text{(R3)}$$

$Cl^•$ is a powerful atmospheric oxidant that can outcompete the hydroxyl radical ($OH^•$, the major atmospheric oxidant) in some cases.[16] For example, $Cl^•$ is more reactive than $OH^•$ toward alkanes.[17] Reactions between $Cl^•$ and VOCs are

Received: September 9, 2020
Revised: January 25, 2021
Accepted: January 29, 2021

important to air quality and the climate as they can result in the production of O_3[5,6,17−19] and SOA.[2]

Most research on $ClNO_2$ chemistry focuses on its production in urban coastal regions where there are large sources of both NO_x from anthropogenic activity and particulate Cl^- from sea spray. However, recent field studies have also observed $ClNO_2$ formation in urban continental regions at concentrations similar to those observed in coastal regions[13,20−23] suggesting that there are other sources of particulate Cl^- that can participate in $ClNO_2$ formation besides sea salt. Sources of inland particulate Cl^- include road salts,[20] swimming pools,[6,24] industrial cooling towers,[6,24] power plants,[23] and biomass burning.[25] Recently, a study by Mitroo et al.[26] identified mineral dust emitted from saline playas (dried saline lakes) as an inland source of Cl-containing aerosols that can participate in $ClNO_2$ chemistry. Mineral dust is not traditionally thought to contain much Cl^-; however, playas have long been known to be disproportionately significant global sources of dust which tend to be saline in composition,[27−29] often producing Cl-containing evaporite minerals such as halite (NaCl).[30]

While Mitroo et al.[26] demonstrated the potential role of playa dust in inland $ClNO_2$ formation, the relationship between playa dust particle chemical composition and $ClNO_2$ production is still poorly understood. Most laboratory studies utilize commercially available standards, including sodium chloride (NaCl), to investigate $ClNO_2$ formation.[5,9,14,31,32] The chemical composition of lab standards is often very simple compared to the chemical complexity of ambient aerosol, requiring assumptions to be made in translating laboratory results to the atmosphere.[20] Further, most studies perform bulk chemical analyses on aerosols when linking particle composition to ϕ_{ClNO2}. The complex chemistry of ambient aerosols is not fully captured by bulk analytical techniques, possibly explaining why $ClNO_2$ production is poorly predicted in many studies,[20] including in the results from Mitroo et al.[26] To better understand the controls on $ClNO_2$ production from chemically complex samples, a more detailed aerosol chemical analysis is required.

In this study, we expand on the research from Mitroo et al.[26] by performing bulk and single-particle analyses of playa sediment and dust samples to elucidate the chemical mechanisms that control the fate of N_2O_5 reacted on playa dust and the subsequent production of $ClNO_2$. Our analyses show that highly hygroscopic magnesium (Mg) and calcium (Ca) Cl-containing minerals, clay minerals, playa sediment organic matter, and surface chemical composition influence the reactivity of N_2O_5 and $ClNO_2$ production from playa dusts. More broadly, our findings also underscore the role of mixing state, competing reactions, and surface chemistry on the efficiency of γ_{N2O5} and ϕ_{ClNO2} with expected relevance in other aerosol systems beyond saline playa dusts. To conclude, we discuss how these results can be used to improve parameterizations of $ClNO_2$ formation.

2. METHODS

In this study, we performed both bulk and single-particle analytical techniques to determine the chemical composition of playas from the Southwestern United States. Techniques utilized include ion chromatography (IC) to determine the bulk soluble ion content of playa sediments, X-ray diffraction (XRD) to determine the bulk mineralogy of playa sediments, scanning electron microscopy coupled with energy dispersive X-ray spectroscopy (SEM/EDX) to determine the elemental composition of individual particles, and finally, single particle mass spectrometry (SPMS) to determine the chemical composition of individual aerosol particles. Results from these analyses were then compared to γ_{N2O5} and ϕ_{ClNO2} values determined by Mitroo et al.[26] to elucidate the effect of particle chemical composition and mineralogy on N_2O_5 uptake and $ClNO_2$ yield.

2.1. Sediment and Dust Sample Collection. As described in Mitroo et al.,[26] sediment samples were collected from dust-emitting saline playas including Black Rock Desert (Nevada), Great Salt Lake (Utah), Lordsburg Playa (New Mexico), Owens (dry) Lake (California), Salt Flat Basin (Texas), Salton Sea (California), and Sulphur Springs Draw (Texas). None of the samples were altered before analysis, except the Great Salt Lake sample, which was wet when collected and then dried at 45 °C for 72 h. All sediment samples were stored in sealed polyethylene containers until analysis.

2.2. Determination of N_2O_5 Uptake and $ClNO_2$ Yields. N_2O_5 uptake coefficients (γ_{N2O5}) and $ClNO_2$ yields (ϕ_{ClNO2}) were determined for submicrometer ($d < 1$ μm) playa dust particles at relative humidities (RHs) ranging from 16% to 51% in flow tube experiments conducted by Mitroo et al.[26] Our analyses here focus on γ_{N2O5} and ϕ_{ClNO2} values determined at 30% RH because all samples were run at this RH value.

All $ClNO_2$ yield and N_2O_5 uptake measurements discussed herein were previously described by Mitroo et al.[26] Aerosols were produced using a custom dry generation system and then reacted in an aerosol flow tube with N_2O_5; a chemical ionization mass spectrometer (CIMS) was used to detect $ClNO_2$ and N_2O_5 and determine the reactive uptake of N_2O_5 (γ_{N2O5}) and the production of $ClNO_2$ per amount of N_2O_5 reacted (e.g., the yield, ϕ_{ClNO2}). Further details regarding the methods are included in Mitroo et al.[26]

2.3. Bulk Analysis. Ion chromatography (IC) was utilized to determine the soluble ion content of the playa sediments. IC was performed as described in Mitroo et al.[26] and Gaston et al.[33] Additional details can be found in the Supporting Information (SI).

Bulk mineralogy, reflective of the mineralogy of all particles in a playa sediment sample, was determined using powder X-ray diffraction (XRD) performed at the U.S. Geological Survey (Reston, VA). Samples were first dry ground with an agate mortar and pestle (to minimize disturbance to evaporite minerals) and then sieved through a 420 μm mesh prior to loading into 30 mm side-loaded aluminum sample holders. Samples were analyzed using a PANalytical X'Pert Pro X-ray diffractometer (type-PW3040, The Netherlands) with 45 kV and 40 nA using CuKα radiation and scanned from 3 to 80° 2θ using 0.0167° steps. Most samples were run at a 60 s dwell time, with the exceptions of the Black Rock and Lordsburg samples, which were run at 600 s to improve the signal-to-noise ratio. Rietveld refinements were performed using X'Pert Highscore Plus software (PANalytical; version 4.7) and the ICSD Database (FIZ Karlsruhe, 2013); additional details on the pattern refinements are available in the SI. We refer to categories of clay minerals based on their basal spacing (e.g., 7 and 10 Å clays), which is defined as the distance from a layer of atoms in a clay mineral plus the interlayer space between them. Further, hand grinding and variability in mineral "crystallinity" in samples combine to limit the accuracy of the Rietveld refinements, meaning that absolute abundances are considered

https://dx.doi.org/10.1021/acs.est.0c06067
Environ. Sci. Technol. XXXX, XXX, XXX−XXX

semiquantitative (see text in the SI for further discussion, Figure S1, and Table S1). Despite these limitations, XRD provides key mineral identification, especially since pattern peak fits were constrained by the results of complementary techniques.

2.4. Single Particle Analysis. The elemental composition of individual playa sediment particles was measured at the University of Miami's Center for Advanced Microscopy (CAM) using a Philips XL-30/ESEM-FED scanning electron microscope coupled with an Oxford Instruments (UK) Ltd. energy dispersive X-ray spectrometer (SEM/EDX). Samples were crushed with an agate mortar and pestle to break up any aggregates and then filtered through a 125 μm mesh. Filtered samples were then applied to carbon-coated copper grids (Ted Pella, Inc.) by first applying the grids to an aluminum stub with a carbon adhesive and then pressing the stub onto a thin layer of dust to adhere particles. Particles were analyzed using an acceleration of 20 kV. For each sample, between 49 and 124 particles with diameter <10 μm were imaged and analyzed for elemental composition. Representative particle images and spectra can be found in SI Figure S2.

The size-resolved chemical composition of individual dust particles was also determined using a single particle aerosol mass spectrometer (Hexin, SPMS 0515).[34] Analyzed playa dust particles were generated using a custom dry aerosol generation set up.[26] Particles with diameters of 0.2 to 1 μm were analyzed by SPMS, based on the instrument's lower size limit of 0.2 μm, and for consistency with the previous uptake experiments that targeted submicrometer particles (e.g., d < 1 μm), which are most likely to undergo long-range atmospheric transport. Briefly, particles entered the single particle mass spectrometer (SPMS) through an aerodynamic lens into a vacuum chamber where particles were accelerated to a size-dependent terminal velocity. Particles were then scattered by two 532 nm continuous wave lasers (CNI, MLL-532−50 mW) located 6 cm apart, which provides a measure of the size-dependent terminal velocity that is converted to the particle vacuum aerodynamic diameter (d_{va}) by calibration with polystyrene latex spheres of known diameter (269, 400, 700, 800, 1000, and 1600 nm). The particle sizing region also initiates a timing circuit, which times the firing of a 266 nm, 20-Hz Nd:YAG laser (Quantel Ultra 50). In this study, the 266 nm laser was operated at ∼0.5 mJ/pulse to induce laser desorption/ionization. Positive and negative ions produced from individual particles were detected using a dual-reflection time-of-flight mass spectrometer. Due to the low laser energy used in our analysis compared to most SPMS studies (typically ∼1−1.5 mJ/pulse), the resulting mass spectra are likely more reflective of the particle surface, rather than the full particle.[35]

Mass spectra were imported into MATLAB (ver 9.6.0; The Mathworks Inc.) and analyzed using a Flexible Analysis Toolkit for the Exploration of Single-particle mass spectrometer data (FATES).[36] Mass spectra were clustered based on the presence and intensity of ion peaks in individual single-particle mass spectra using an Adaptive Resonance Theory-based neural network algorithm (ART-2a) at a vigilance factor of 0.8. "Clusters" are then merged into distinct particle types based on the prevalent mass spectral ions and intensities, which are indicative of particle sources and chemistry and reflect over 25 years of analysis using SPMS, including analysis of dust particles.[37−40] A discussion of the characteristics of each particle type, representative spectra of each sample (SI Figure S3), and representative spectra of particle types (SI Figure S4) can be found in the SI. In addition to particle types, we also determined the relative amount of specific chemical species using the average peak areas of specific ions.[41,42]

Carbonates were expected to be a major particle type in the SPMS analysis based on the high mass percentage of carbonate mineral content of some of the playa sediments from XRD analysis. However, the SPMS is not sensitive to carbonates due to the desorption/ionization laser wavelength.[33,40] In order to compare SPMS and XRD results, SPMS number concentrations were scaled, following documented methods,[43,44] to account for undetected carbonates, resulting in a "missed particles" category in descriptions of samples from SPMS analysis (see SI for a detailed discussion of the scaling procedure, Figure S5 for scaled results, and Figure S6 for hit rates used to scale the data).

3. RESULTS AND DISCUSSION

Silicate minerals, Cl-containing minerals, and organic material in playa sediments are prevalent in our dust samples and affect N_2O_5 uptake and $ClNO_2$ production from playa dusts. Results from IC, SPMS, SEM/EDX, and XRD complement one another and provide unique insights into particle composition as well as highlight key chemical differences at the single-particle level and on particle surfaces that differ from the average bulk composition. Here, we only provide descriptions of playa dust chemical composition which are essential for understanding our results; however, a detailed description of the composition of the samples studied is provided in the SI.

3.1. Hygroscopic Cl-Containing Minerals Enhance $ClNO_2$ Production at Low Humidity. Our results show that highly hygroscopic magnesium (Mg) and calcium (Ca) Cl-containing minerals are present in trace quantities, and likely facilitate $ClNO_2$ formation at low (e.g., 30%) RH. Figure 1a presents ϕ_{ClNO2} determined at 30% RH compared to the number fraction of particles analyzed with SEM/EDX containing no detectable Cl, Cl with Na (halite), and Cl without detectable Na. Examples of each particle type can be found in SI Figure S2. Previous work has primarily focused on halite in sea spray aerosol as the major source of Cl-containing aerosol responsible for $ClNO_2$ formation.[14,45,46] From XRD (SI Table S1) and SPMS (SI Table S2) analyses, halite is the dominant source of Cl in the samples analyzed in this study, suggesting it should be the most important mineral for $ClNO_2$ formation from playa dust. However, if halite were the major important mineral for $ClNO_2$ formation on playa dust, then ϕ_{ClNO2} in Figure 1a should correlate with particles containing both Cl and Na; surprisingly, scatter plots in Figure 1b comparing ϕ_{ClNO2} with the number percentage of particles containing both Cl and Na show a very poor correlation (R^2 = 0.07). Further, Sulphur Springs and Salt Flat would be expected to have the lowest ϕ_{ClNO2} considering they have the lowest number fraction of particles with Cl and Na (excluding Lordsburg). However, they have the highest ϕ_{ClNO2}.

Figure 1a indicates that ϕ_{ClNO2} is more directly related to particles containing Cl without detectable Na demonstrating that minerals other than halite are more important for $ClNO_2$ formation at 30% RH. Indeed, the scatter plot shown in Figure 1c comparing ϕ_{ClNO2} with the number percentage of particles containing Cl but no detectable Na shows a very strong correlation (R^2 = 0.63). Overall, the strong correlation shown in Figure 1d (R^2 = 0.68), which compares ϕ_{ClNO2} with the number percentage of all particles containing Cl, is mainly determined by particles containing Cl with no detectable Na

https://dx.doi.org/10.1021/acs.est.0c06067
Environ. Sci. Technol. XXXX, XXX, XXX−XXX

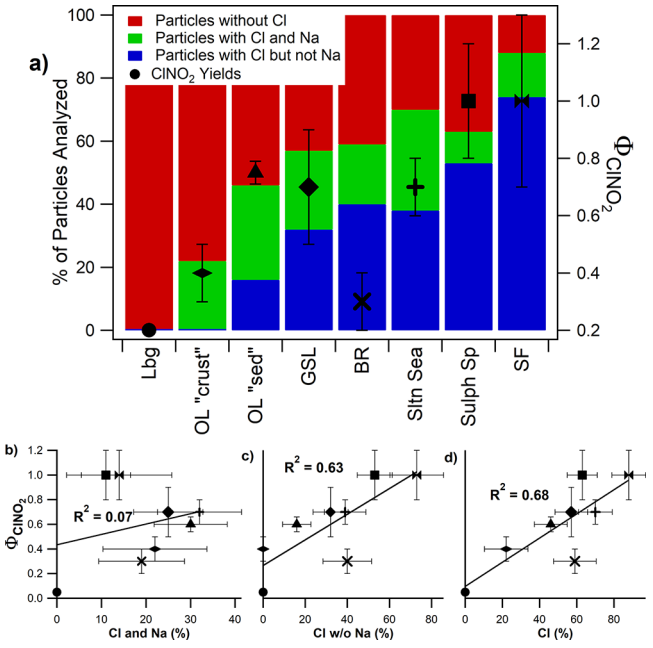

Figure 1. (a) Number percentage of particles (<10 μm in diameter) analyzed by SEM/EDX that contained no detectable Cl (red), Cl and Na (green), and Cl but no detectable Na (blue) compared to ϕ_{ClNO2} measured at 30% RH (ϕ_{ClNO2}; black dots; determined by Mitroo et al.[26]) for Lordsburg (Lbg), Owens Lake "crust" (OL "crust"), Owens Lake "sediment" (OL "sed"), Great Salt Lake (GSL), Black Rock (BR), Salton Sea (Sltn Sea), Sulphur Springs (Sulph Sp), and Salt Flat (SF). Correlation plots compare ϕ_{ClNO2} to the number percentages of measured particles (b) containing Cl and Na, (c) Cl but no detectable Na, and (d) all particles containing Cl. Trendlines within correlation plots are all least-squares fit regressions. Error bars in ϕ_{ClNO2} represent one standard deviation and 95% confidence intervals for number percentages of particles.

that are indicative of nonhalite Cl-containing minerals. In addition to the SEM/EDX results shown in Figure 1, XRD also detected Cl-containing minerals other than halite, including sylvite (KCl; detected in Great Salt Lake, Owens Lake "sediment", Salt Flat, and Lordsburg samples), as well as carnallite ($KCl{\cdot}MgCl_2{\cdot}2H_2O$; detected in Owens Lake "sediment"). SPMS analysis also suggests that Black Rock, Salt Flat, Salton Sea, and Owens Lake "crust" contain sylvite due to the presence of $^{113,115}K_2Cl^+$ ion peaks. SPMS also detected ions indicative of calcium chloride and magnesium chloride minerals including $^{145,147}CaCl_3^-$, $^{129,131,133}MgCl_3^-$, $^{127,129,131}CaCl_2OH^-$, $^{75,77,79,81}CaCl^+$, and $^{131,133}Ca_2OCl^+$ (see SI Table S2). The detection of calcium chloride and magnesium chloride ions from SPMS and particles with Cl but no detectable Na from SEM/EDX (both single particle techniques) indicates that single particle analyses are more effective at detecting trace Cl-containing minerals than bulk techniques, such as XRD and IC, which are only capable of detecting major mineral constituents and bulk ion content, respectively.

The hygroscopic nature of Cl-containing minerals other than halite is also important for providing deliquesced forms of chloride at 30% RH in order for efficient $ClNO_2$ formation to occur.[5,32,45,47] Many magnesium chloride and calcium chloride minerals like bischofite ($MgCl_2{\cdot}6H_2O$; DRH = 33%[48]) and antarcticite ($CaCl_2{\cdot}6H_2O$; DRH = 12−20%[49]) are more hygroscopic than halite. Although rare in nature, these minerals have been found in higher concentrations in some terrestrial playa brines,[50,51] and results of our chemical and mineralogical analyses suggest that these minerals are present in our samples as well and, even in trace quantities, likely explain the high ϕ_{ClNO2} observed at low (30%) RH.

3.2. Impact of Competing Reactions on γ_{N2O5} and ϕ_{ClNO2}. Unexpected trends in γ_{N2O5} and ϕ_{ClNO2} can also be explained by the presence of clay minerals and organic matter associated with playa sediments. Though Figure 1 shows a clear trend between particles "with Cl but no detectable Na" and ϕ_{ClNO2}, Black Rock does not fit into this trend. This sample has a high number fraction of particles "with Cl but no detectable Na", yet ϕ_{ClNO2} at 30% RH is much lower (ϕ_{ClNO2} = 0.3 ± 0.1) than samples like Great Salt Lake (ϕ_{ClNO2} = 0.7 ± 0.2) and Salton Sea (ϕ_{ClNO2} = 0.7 ± 0.1), which have similar percentages of hygroscopic minerals. Also anomalous is its high γ_{N2O5} at 30% RH (γ_{N2O5} = 0.072 ± 0.005) compared to samples like Sulphur Springs (γ_{N2O5} = 0.030 ± 0.010) and Salt Flat (γ_{N2O5} = 0.020 ± 0.005), which have γ_{N2O5} similar to that of halite (γ_{N2O5} = 0.03).[14,31,45,52] XRD analysis revealed that nearly all samples (except Owens Lake "crust" and Salt Flat) contained detectable amounts of 10 Å-clays, which include minerals such as primary micas (biotite ($K(Mg,Fe^{2+})_3(AlSi_3O_{10}(OH,F)_2)$) and muscovite ($KAl_2(Si_3,Al)O_{10}(OH,F)_2)$), and their initial weathering product, Illite ($(K,H_3O)(Al,Mg,Fe)_2(Si,Al)_4O_{10}[(OH)_2,(H_2O)]$), which has been demonstrated to be reactive with N_2O_5. XRD indicated that Black Rock and Lordsburg samples contained the highest concentrations of 10 Å clay minerals at 11% by mass (SI Table S1). These samples also have some of the highest γ_{N2O5} at 0.072 ± 0.005 and 0.077 ± 0.017 and the lowest ϕ_{ClNO2} at 0.3 ± 0.1 and 0.05 ± 0.01, respectively.

The effect of 10 Å clays on γ_{N2O5} and ϕ_{ClNO2} for all samples is depicted in Figure 2. Figure 2a shows that as the mass

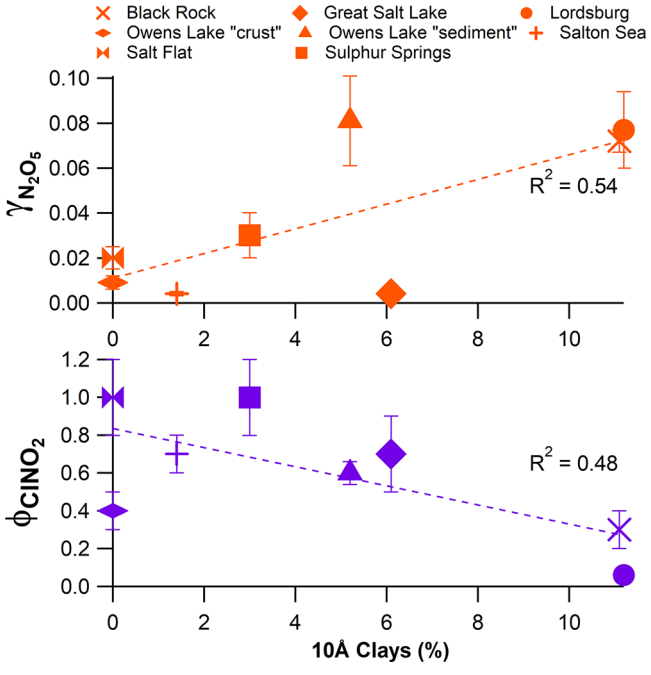

Figure 2. γ_{N2O5} and ϕ_{ClNO2} (determined at ~30% RH by Mitroo et al.[26]) plotted against 10 Å clay mass percent determined by XRD. Error bars represent one standard deviation. Dotted lines represent least-squares fit trendlines. Marker symbols represent the same samples as they do in Figure 1.

https://dx.doi.org/10.1021/acs.est.0c06067
Environ. Sci. Technol. XXXX, XXX, XXX−XXX

concentration of 10 Å clays increases, γ_{N2O5} also increases (R^2 = 0.54). Figure 2b shows that ϕ_{ClNO2} decreases with an increase in the mass concentration of 10 Å clays (R^2 = 0.48). We also see similar trends when comparing γ_{N2O5} and ϕ_{ClNO2} to ion peaks in the SPMS data indicative of clay minerals, highlighting the robustness of this finding (see SI Figure S7). These trends are best explained by clay mineral surfaces outcompeting Cl-containing minerals for N_2O_5, particularly at low RH. Previous research has shown that N_2O_5 is highly reactive on mineral dust.[53] Specifically, the common mineral dust constituent Illite has been shown to be highly effective at reacting with N_2O_5 at low RH, but less effective at high RH.[54] Mitroo et al.[26] saw a similar γ_{N2O5} trend with Black Rock dust where γ_{N2O5} consequently decreased from 0.072 ± 0.005 to 0.022 ± 0.002 as RH was increased from 29% to 49%. From Figure 2a, we confirm that this trend can be explained by reactions between N_2O_5 and clay minerals, which are hypothesized to be more efficient than hydrolysis at low RH.[55,56] We also show in Figure 2b that as 10 Å clay mass concentrations increase, more N_2O_5 will react with these minerals over Cl^-, which results in a high γ_{N2O5} and low ϕ_{ClNO2}.

To our knowledge, this is the first work to show that clays not only react with N_2O_5 more efficiently than water, but they also react with N_2O_5 more efficiently than chloride at low RH. As RH increases, it is likely that a water layer forms on the surface of the particle, at which point the hydrolysis reaction is preferred over the N_2O_5-clay reaction, leading to a decrease in γ_{N2O5}.[54,56] We propose that this water layer also dissolves Cl-containing minerals resulting in aqueous Cl^- formation, which can then react with N_2O_5 to form $ClNO_2$ and increase ϕ_{ClNO2} as RH increases. The competition between water, chloride, and surficial OH groups present in clays for N_2O_5 likely explains several of our trends in ϕ_{ClNO2} and γ_{N2O5} as a function of RH.

Salton Sea is also anomalous because of its low γ_{N2O5} (0.004−0.006) at all RHs studied in Mitroo et al.[26] (16−46%). This trend is especially interesting because both bulk and single-particle analyses indicate that Salton Sea has the highest Cl^- content. Figure 1 shows that Salton Sea has the second highest number fraction of particles containing Cl^- ("particles with Cl and Na + particles with Cl but no Na") at 71% by number, second only to Salt Flat at 87% by number. XRD data determined that Salton Sea had the highest halite content (23% by mass) (SI Table S1 and Figure S1). Finally, results from SPMS analysis show that Salton Sea had the highest number fraction of particles dominated by Cl^- salts including several calcium chloride and magnesium chloride compounds, which indicate the presence of highly hygroscopic Cl-containing minerals. These results all suggest that Salton Sea contains Cl-containing minerals that should react efficiently with N_2O_5 and produce high ϕ_{ClNO2}. However, as demonstrated in Mitroo et al.,[26] γ_{N2O5} for this sample ranged from only 0.004 ± 0.001 to 0.006 ± 0.001 (almost an order of magnitude below γ_{N2O5} of halite at γ = 0.03), while its ϕ_{ClNO2} mimics that of pure halite as it increases from 0.2 ± 0.1 to 0.7 ± 0.3 with an increase in RH from 16% to 46%.[26]

The most likely explanation for the trends observed for the Salton Sea is the presence of organic material in our playa sediment samples, which blocks N_2O_5 from reacting with the dust but does not lower ϕ_{ClNO2}. Figure 3 compares the average SPMS peak area for $^{42}CNO^-$ and $^{26}CN^-$ − ions which indicate the presence of nitrogen-containing organic matter from sediments and soils − to γ_{N2O5} values from Mitroo et al.[26]

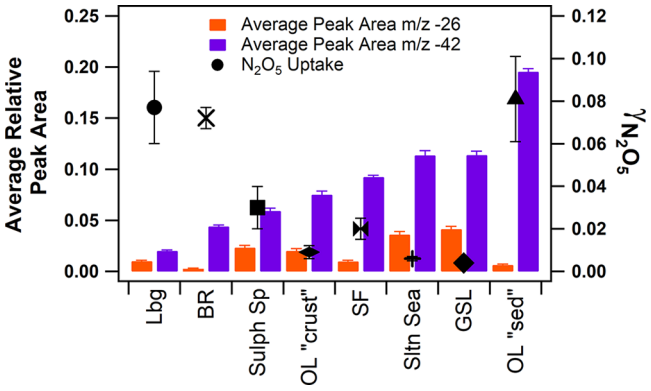

Figure 3. Average SPMS relative peak areas of $^{26}CN^-$ (orange bar) and $^{42}CNO^-$ (purple bar) and γ_{N2O5} (black dots; determined at ~30% by Mitroo et al.[26]) plotted for each playa dust sample including Lordsburg (Lbg), Black Rock (BR), Sulphur Springs (Sulph Sp), Owens Lake "crust" (OL "crust"), Salt Flat (SF), Salton Sea (Sltn Sea), Great Salt Lake (GSL), and Owens Lake "sediment" (OL "sed"). Error bars represent one standard deviation. Marker symbols represent the same samples as they do in Figure 1.

Previous research utilizing SPMS to analyze soil organic matter consistently detected these two organonitrogen peaks.[38,43,57,58] The plot shows an inverse relationship where an increase in $^{42}CNO^-$ peak area corresponds to a decrease in γ_{N2O5}. The exception to this trend is the Owens Lake "sediment" sample where SPMS detected the highest average $^{42}CNO^-$ peak areas, yet it has a high γ_{N2O5} of 0.081 ± 0.020. This sample is likely an outlier due to the presence of bromide,[26] as this sample had a γ_{N2O5} similar to that of bromide-containing salts.[26,59] Previous research has shown that surface-active organics can impede N_2O_5 uptake by coating the surface of a particle and preventing N_2O_5 from reacting with other constituents.[45,52,60,61] However, no studies have looked at the effect of organic matter in playa sediments or other dusts on N_2O_5 uptake, even though it is a common constituent of dust aerosols.[43,57,58] We propose that organic matter in playa sediments coats playa particles and prevents N_2O_5 from reacting with other playa sediment constituents. This results in low γ_{N2O5} and a high ϕ_{ClNO2}. To our knowledge, this is the first study to show that organic matter in playa sediment can diminish N_2O_5 uptake in a similar manner to previously studied surfactants and SOA.

3.3. The Importance of the Particle Surface Composition for $ClNO_2$. The results from bulk and single-particle techniques suggest that ϕ_{ClNO2} is determined by surface chemistry. Figure 4 contains two plots that show ϕ_{ClNO2} for each sample plotted against Cl^- mass concentrations from IC analysis (Figure 4a) and average SPMS $^{81}Na_2Cl^+$ absolute peak areas—reflective of the halite content of individual particles—from the most representative cluster of each sample analyzed by SPMS (Figure 4b). IC is a bulk analytical technique, while SPMS is a single-particle method that, in this study, is more reflective of the particle surface due to the low laser energy used in our analysis.[35]

Figure 4a shows little to no relationship between bulk Cl^- mass concentrations in playa sediments and ϕ_{ClNO2} (R^2 = 0.17). In contrast, Figure 4b shows two distinct relationships between SPMS $^{81}Na_2Cl^+$ peak areas and ϕ_{ClNO2}: a high-slope trend (m = 0.0019; R^2 = 0.89) in which little $^{81}Na_2Cl^+$ is required to produce a high ϕ_{ClNO2} and a low-slope trend (m = 0.0003; R^2 = 0.97), where high $^{81}Na_2Cl^+$ content leads to

https://dx.doi.org/10.1021/acs.est.0c06067
Environ. Sci. Technol. XXXX, XXX, XXX−XXX

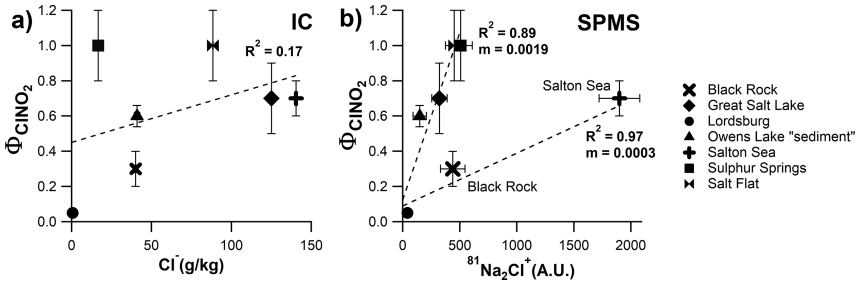

Figure 4. Correlation plots comparing ϕ_{ClNO2} (determined at 30% RH by Mitroo et al.[26]) to (a) [Cl^-] from bulk IC analysis and (b) absolute peak areas of $^{81}Na_2Cl^+$ from SPMS analysis. Dotted lines represent least-squares fit trendlines for the SPMS plot and "m" denotes the slope of the trendlines in plot (b). The Owens Lake "crust" sample is excluded due to the low data collection rate (see SI for more detail). Marker symbols represent the same samples as they do in Figure 1.

moderate increases in ϕ_{ClNO2}. The high-slope trend includes the Owens Lake "sediment", Sulphur Springs, Salt Flat, and Great Salt Lake. Results from all chemical analyses performed on these samples suggest that they contain highly hygroscopic Cl-containing minerals, implying that the Cl^- reaction pathway is highly efficient for these samples; therefore, low average SPMS peak areas of $^{81}Na_2Cl^+$ can be correlated to high ϕ_{ClNO2}. In the low-slope trend, Black Rock and Salton Sea have high average SPMS absolute peak areas of $^{81}Na_2Cl^+$ with unexpectedly low ϕ_{ClNO2}. Single particle chemical analyses suggest that these samples contain highly hygroscopic Cl-containing minerals, perhaps including bischofite ($MgCl_2 \cdot 6H_2O$) or even calcium chlorides, that should facilitate $ClNO_2$ formation at 30% RH; however, these are the same samples that contain competing chemical constituents such as clays and playa sediment organic matter. As discussed, these compounds interfere with the reaction between N_2O_5 and Cl^-, which impedes $ClNO_2$ production even if Cl^- content is high. To show the effect of clay minerals in Black Rock on ϕ_{ClNO2}, SI Figure S8 presents the same SPMS $^{81}Na_2Cl^+$ data as Figure 4b normalized to the average SPMS peak area of m/z −76 (commonly representative of $^{76}SiO_3^-$ and occasionally $^{76}AlO_2(OH)_2^-$), a peak which is indicative of aluminosilicate minerals. When the data are normalized to the clay content in each sample, the Black Rock sample fits better into the high-slope trend compared to the low-slope trend, further supporting the claim that clays are the reason that Black Rock does not produce as much $ClNO_2$ as expected considering its Cl^- content.

These clear trends in the SPMS plot compared to the absence of any trends in the IC plot also suggest that $ClNO_2$ formation on playa dusts can be considered a surface chemical reaction as suggested by previous gas-phase kinetics studies.[31] Our results also agree with a recent study, which showed that single-particle composition is more effective at predicting $ClNO_2$ formation than bulk aerosol composition.[20]

4. ATMOSPHERIC IMPLICATIONS

In this study, we found that several factors beyond traditionally considered parameters (e.g., bulk chloride content and predicted aerosol liquid water content) affect ϕ_{ClNO2}. Surface and bulk analyses show that highly hygroscopic Cl-containing evaporite minerals, likely hydrated magnesium or calcium chlorides, are present and facilitate $ClNO_2$ formation at low RH even in trace quantities. We also found that competing chemical constituents, such as clay minerals, can outcompete Cl^- for N_2O_5 and diminish ϕ_{ClNO2}. This finding robustly shows a relationship between particle clay mineral content and increases in γ_{N2O5}, providing more definitive proof that clays react more efficiently with N_2O_5 than water. Other competing chemical constituents, such as organic material in playa sediments, also hinder the reactive uptake of N_2O_5. This finding further emphasizes the ability of primary organic aerosols to hinder the reactive uptake of trace gases. Finally, comparisons between Cl-content and ϕ_{ClNO2} from bulk and surface analytical techniques suggest that N_2O_5 reacts more efficiently with surface Cl^- content rather than bulk Cl^- content.

Though we show how playa composition affects $ClNO_2$ yields and N_2O_5 reactivity, our findings have broader impacts for understanding heterogeneous reactions on different gas-particle systems. Highly hygroscopic compounds, organic matter, and competing constituents are widely found in ambient aerosols beyond those emitted from playas.[62] Hence, our findings also highlight the applicability of these methods and results to understand other heterogeneous reactions on ambient aerosols.

This work is also among the few laboratory studies to probe $ClNO_2$ chemistry using authentic environmental samples rather than model systems. Previous research has already shown that clays[54] and organics[52] affect N_2O_5 reactivity using commercially available standards, which are useful for understanding the effect of particular compounds on $ClNO_2$ formation. However, these materials lack the chemical complexity of environmental samples. The results from our study can therefore augment laboratory studies that use commercial standards. By studying chemically complex sediment samples, we were able to elucidate the relationships between various chemical components in an aerosol and their combined effect on ϕ_{ClNO2}.

While traditional parameterizations of $ClNO_2$ formation provided an important foundation for predicting $ClNO_2$ production, they do not include the chemical complexity that we show affects $ClNO_2$ formation.[14,63] This traditional parameterization relies on Cl-concentrations from bulk methods, namely IC, to predict $ClNO_2$ formation. However, our results show that surface chemistry is a more important predictor of $ClNO_2$ formation than bulk chemistry. The distribution of clays, organics, and trace quantities of highly hygroscopic Cl-containing compounds, constituents that compete for N_2O_5, across the particle population must be considered. This finding, and those from similar recent studies,[20,21,23,64−66] demonstrate that simulation of $ClNO_2$ needs to take into account the effect of particle surface composition on $ClNO_2$ formation in order to accurately predict the impact of this chemistry on air quality.

https://dx.doi.org/10.1021/acs.est.0c06067
Environ. Sci. Technol. XXXX, XXX, XXX−XXX

Recently, McNamara et al. demonstrated the value of incorporating particle surface composition into the simulation of $ClNO_2$ by developing a new "single-particle" parametrization that uses particle type-specific ϕ_{ClNO2} and γ_{N2O5} values, which are weighted according to the surface area concentrations of various particle types.[20] The ϕ_{ClNO2} and γ_{N2O5} values used in this parameterization are assigned to ambient particle types based on comparison to laboratory aerosol proxies. Therefore, the results of our laboratory study can directly be applied to this parameterization, for improved simulation of $ClNO_2$ production in arid regions impacted by playa dust emissions, including Salt Lake City, Utah, where multiple salt sources complicate the simulation of $ClNO_2$.[67] To reduce the uncertainty associated with the application of this parameterization, further studies of complex model aerosol systems and authentic aerosols, such as those probed herein, are needed to obtain realistic ϕ_{ClNO2} and γ_{N2O5} values for application in this new single-particle parameterization. Overall, our results show that understanding the complex chemistry and heterogeneity of aerosol surface composition is essential for understanding and simulating $ClNO_2$ formation and impacts on air quality.

■ ASSOCIATED CONTENT

Supporting Information

The Supporting Information is available free of charge at https://pubs.acs.org/doi/10.1021/acs.est.0c06067.

Description of ion chromatography analysis methods, X-ray diffraction data processing, additional details on playa dust chemistry, and correction of single particle mass spectrometry data for missing carbonates, eight figures (XRD waterfall plot, SEM/EDX sample images and spectra, representative SPMS spectra, pie charts of each particle type detected by SPMS, hit rate histograms from SPMS, and comparisons of γ_{N2O5} and ϕ_{ClNO2} to SPMS average relative peak areas), and two tables (XRD analysis results and Cl-containing ions detected using SPMS) are included therein (PDF)

■ AUTHOR INFORMATION

Corresponding Author

Cassandra J. Gaston − *Department of Atmospheric Sciences, Rosenstiel School of Marine and Atmospheric Science, University of Miami, Miami, Florida 33149, United States;* orcid.org/0000-0003-1383-8585; Phone: (305)-421-4979; Email: cgaston@rsmas.miami.edu

Authors

Haley M. Royer − *Department of Atmospheric Sciences, Rosenstiel School of Marine and Atmospheric Science, University of Miami, Miami, Florida 33149, United States;* orcid.org/0000-0002-0481-4496

Dhruv Mitroo − *Department of Atmospheric Sciences, Rosenstiel School of Marine and Atmospheric Science, University of Miami, Miami, Florida 33149, United States;* orcid.org/0000-0002-7398-2020

Sarah M. Hayes − *U.S. Geological Survey, Geology, Energy, and Minerals Science Center, Reston, Virginia 20192, United States;* orcid.org/0000-0001-5887-6492

Savannah M. Haas − *Department of Chemistry, University of Michigan, Ann Arbor, Michigan 48109, United States*

Kerri A. Pratt − *Department of Chemistry, University of Michigan, Ann Arbor, Michigan 48109, United States;* orcid.org/0000-0003-4707-2290

Patricia L. Blackwelder − *Center for Advanced Microscopy (UMCAM), Department of Chemistry and Department of Marine Geological Sciences, Rosenstiel School of Marine and Atmospheric Science, University of Miami, Coral Gables, Florida 33146, United States*

Thomas E. Gill − *Environmental Science and Engineering Program and Department of Geological Sciences, University of Texas at El Paso, El Paso, Texas 79968, United States;* orcid.org/0000-0001-9011-4105

Complete contact information is available at: https://pubs.acs.org/10.1021/acs.est.0c06067

Notes

The authors declare no competing financial interest.

■ ACKNOWLEDGMENTS

The research presented in this paper is supported by National Science Foundation grants (AGS-1663740 and AGS-1663726). S.H. and K.A.P. acknowledge the University of Michigan REU Program in Chemical Sciences (CHE-1460990). We are also grateful to the following individuals for collecting some of the samples: Professor Heather Holmes and Professor Bernhard Bach; Professor Maura Hahnenberger; Professor Joanna Nield, Jana Lasser, and Lucas Goehring; Professor Junran Li; Professor Roya Bahreini; Dr. R. Scott Van Pelt. Any use of trade, product, or firm names in this publication is for descriptive purposes only and does not imply endorsement by the U.S. Government.

■ REFERENCES

(1) Simpson, W. R.; Brown, S. S.; Saiz-Lopez, A.; Thornton, J. A.; von Glasow, R. Tropospheric halogen chemistry: Sources, cycling, and impacts. *Chem. Rev.* **2015**, *115* (10), 4035−4062.

(2) Wang, D. S.; Ruiz, L. H. Secondary organic aerosol from chlorine-initiated oxidation of isoprene. *Atmos. Chem. Phys.* **2017**, *17* (22), 13491−13508.

(3) Jimenez, J. L.; Canagaratna, M.; Donahue, N.; Prevot, A.; Zhang, Q.; Kroll, J. H.; DeCarlo, P. F.; Allan, J. D.; Coe, H.; Ng, N. Evolution of organic aerosols in the atmosphere. *Science* **2009**, *326* (5959), 1525−1529.

(4) Kanakidou, M.; Seinfeld, J.; Pandis, S.; Barnes, I.; Dentener, F. J.; Facchini, M. C.; Dingenen, R. V.; Ervens, B.; Nenes, A.; Nielsen, C. Organic aerosol and global climate modelling: a review. *Atmos. Chem. Phys.* **2005**, *5* (4), 1053−1123.

(5) Behnke, W.; George, C.; Scheer, V.; Zetzsch, C. Production and decay of $ClNO_2$ from the reaction of gaseous N_2O_5 with NaCl solution: Bulk and aerosol experiments. *J. Geophys. Res., [Atmos.]* **1997**, *102* (D3), 3795−3804.

(6) Chang, S.; Allen, D. T. Atmospheric chlorine chemistry in southeast Texas: Impacts on ozone formation and control. *Environ. Sci. Technol.* **2006**, *40* (1), 251−262.

(7) Lawler, M.; Finley, B.; Keene, W.; Pszenny, A.; Read, K.; Von Glasow, R.; Saltzman, E., Pollution-enhanced reactive chlorine chemistry in the eastern tropical Atlantic boundary layer. *Geophys. Res. Lett.* **2009**, *36*, (8). DOI: 10.1029/2008GL036666

(8) Platt, U.; Allen, W.; Lowe, D. Hemispheric average Cl atom concentration from $^{13}C/^{12}C$ ratios in atmospheric methane. *Atmos. Chem. Phys.* **2004**, *4* (9/10), 2393−2399.

(9) Finlayson-Pitts, B.; Ezell, M.; Pitts, J. Formation of chemically active chlorine compounds by reactions of atmospheric NaCl particles with gaseous N_2O_5 and $ClONO_2$. *Nature* **1989**, *337* (6204), 241−244.

(10) Dentener, F. J.; Crutzen, P. J. Reaction of N_2O_5 on tropospheric aerosols: Impact on the global distributions of NO_x, O_3, and OH. *J. Geophys. Res., [Atmos.]* **1993**, *98* (D4), 7149−7163.
(11) Mozurkewich, M.; Calvert, J. G. Reaction probability of N_2O_5 on aqueous aerosols. *J. Geophys. Res.* **1988**, *93* (D12), 15889−15896.
(12) Roberts, J. M.; Osthoff, H. D.; Brown, S. S.; Ravishankara, A.; Coffman, D.; Quinn, P.; Bates, T., Laboratory studies of products of N_2O_5 uptake on Cl− containing substrates. *Geophys. Res. Lett.* **2009**, *36*, (20). DOI: 10.1029/2009GL040448
(13) Thornton, J. A.; Kercher, J. P.; Riedel, T. P.; Wagner, N. L.; Cozic, J.; Holloway, J. S.; Dubé, W. P.; Wolfe, G. M.; Quinn, P. K.; Middlebrook, A. M. A large atomic chlorine source inferred from mid-continental reactive nitrogen chemistry. *Nature* **2010**, *464* (7286), 271−274.
(14) Bertram, T.; Thornton, J. Toward a general parameterization of N_2O_5 reactivity on aqueous particles: the competing effects of particle liquid water, nitrate and chloride. *Atmos. Chem. Phys.* **2009**, *9* (21), 8351−8363.
(15) Ganske, J.; Berko, H.; Finlayson-Pitts, B. Absorption cross sections for gaseous $ClNO_2$ and Cl_2 at 298 K: Potential organic oxidant source in the marine troposphere. *J. Geophys. Res.* **1992**, *97* (D7), 7651−7656.
(16) Haskins, J. D.; Lopez-Hilfiker, F. D.; Lee, B. H.; Shah, V.; Wolfe, G. M.; DiGangi, J.; Fibiger, D.; McDuffie, E. E.; Veres, P.; Schroder, J. C.; Campuzano-Jost, P.; Day, D. A.; Jimenez, J. L.; Weinheimer, A.; Sparks, T.; Cohen, R. C.; Campos, T.; Sullivan, A.; Guo, H.; Weber, R.; Dibb, J.; Green, J.; Fiddler, M.; Bililign, S.; Jaeglé, L.; Brown, S. S.; Thornton, J. A. Anthropogenic Control Over Wintertime Oxidation of Atmospheric Pollutants. *Geophys. Res. Lett.* **2019**, *46* (24), 14826−14835.
(17) Finlayson-Pitts, B. Chlorine atoms as a potential tropospheric oxidant in the marine boundary layer. *Res. Chem. Intermed.* **1993**, *19* (3), 235−249.
(18) Knipping, E. M.; Dabdub, D. Impact of chlorine emissions from sea-salt aerosol on coastal urban ozone. *Environ. Sci. Technol.* **2003**, *37* (2), 275−284.
(19) Tanaka, P. L.; Oldfield, S.; Neece, J. D.; Mullins, C. B.; Allen, D. T. Anthropogenic sources of chlorine and ozone formation in urban atmospheres. *Environ. Sci. Technol.* **2000**, *34* (21), 4470−4473.
(20) McNamara, S. M.; Kolesar, K. R.; Wang, S.; Kirpes, R. M.; May, N. W.; Gunsch, M. J.; Cook, R. D.; Fuentes, J. D.; Hornbrook, R. S.; Apel, E. C. Observation of Road Salt Aerosol Driving Inland Wintertime Atmospheric Chlorine Chemistry. *ACS Cent. Sci.* **2020**, *6* (5), 684−694.
(21) Mielke, L.; Stutz, J.; Tsai, C.; Hurlock, S.; Roberts, J.; Veres, P.; Froyd, K.; Hayes, P.; Cubison, M.; Jimenez, J. Heterogeneous formation of nitryl chloride and its role as a nocturnal NO_x reservoir species during CalNex-LA 2010. *J. Geophys. Res.: Atmos.* **2013**, *118* (18), 10,638−10,652.
(22) Mielke, L. H.; Furgeson, A.; Osthoff, H. D. Observation of $ClNO_2$ in a mid-continental urban environment. *Environ. Sci. Technol.* **2011**, *45* (20), 8889−8896.
(23) Riedel, T. P.; Wagner, N. L.; Dubé, W. P.; Middlebrook, A. M.; Young, C. J.; Öztürk, F.; Bahreini, R.; VandenBoer, T. C.; Wolfe, D. E.; Williams, E. J. Chlorine activation within urban or power plant plumes: Vertically resolved $ClNO_2$ and Cl_2 measurements from a tall tower in a polluted continental setting. *J. Geophys. Res., [Atmos.]* **2013**, *118* (15), 8702−8715.
(24) Tanaka, P. L.; Riemer, D. D.; Chang, S.; Yarwood, G.; McDonald-Buller, E. C.; Apel, E. C.; Orlando, J. J.; Silva, P. J.; Jimenez, J. L.; Canagaratna, M. R. Direct evidence for chlorine-enhanced urban ozone formation in Houston, Texas. *Atmos. Environ.* **2003**, *37* (9−10), 1393−1400.
(25) Ahern, A. T.; Goldberger, L.; Jahl, L.; Thornton, J.; Sullivan, R. C. Production of N_2O_5 and $ClNO_2$ through Nocturnal Processing of Biomass-Burning Aerosol. *Environ. Sci. Technol.* **2018**, *52* (2), 550−559.
(26) Mitroo, D.; Gill, T. E.; Haas, S.; Pratt, K. A.; Gaston, C. J. $ClNO_2$ production from N_2O_5 uptake on saline playa dusts: New insights into potential inland sources of $ClNO_2$. *Environ. Sci. Technol.* **2019**, *53* (13), 7442−7452.
(27) Bullard, J. E.; Harrison, S. P.; Baddock, M. C.; Drake, N.; Gill, T. E.; McTainsh, G.; Sun, Y., Preferential dust sources: A geomorphological classification designed for use in global dust-cycle models. *J. Geophys. Res.* **2011**, *116*, (F4). DOI: 10.1029/2011JF002061
(28) Gill, T. E. Eolian sediments generated by anthropogenic disturbance of playas: human impacts on the geomorphic system and geomorphic impacts on the human system. *Geomorphology* **1996**, *17* (1−3), 207−228.
(29) Hassani, A.; Azapagic, A.; D'Odorico, P.; Keshmiri, A.; Shokri, N. Desiccation crisis of saline lakes: A new decision-support framework for building resilience to climate change. *Sci. Total Environ.* **2020**, *703*, 134718.
(30) Yechieli, Y.; Wood, W. W. Hydrogeologic processes in saline systems: playas, sabkhas, and saline lakes. *Earth-Sci. Rev.* **2002**, *58* (3−4), 343−365.
(31) Gaston, C. J.; Thornton, J. A. Reacto-diffusive length of N_2O_5 in aqueous sulfate-and chloride-containing aerosol particles. *J. Phys. Chem. A* **2016**, *120* (7), 1039−1045.
(32) Stewart, D. J.; Griffiths, P.; Cox, R. Reactive uptake coefficients for heterogeneous reaction of N_2O_5 with submicron aerosols of NaCl and natural sea salt. *Atmos. Chem. Phys.* **2004**, *4* (5), 1381−1388.
(33) Gaston, C. J.; Pratt, K. A.; Suski, K. J.; May, N. W.; Gill, T. E.; Prather, K. A. Laboratory studies of the cloud droplet activation properties and corresponding chemistry of saline playa dust. *Environ. Sci. Technol.* **2017**, *51* (3), 1348−1356.
(34) Li, L.; Huang, Z.; Dong, J.; Li, M.; Gao, W.; Nian, H.; Fu, Z.; Zhang, G.; Bi, X.; Cheng, P. Real time bipolar time-of-flight mass spectrometer for analyzing single aerosol particles. *Int. J. Mass Spectrom.* **2011**, *303* (2−3), 118−124.
(35) Ault, A. P.; Guasco, T. L.; Ryder, O. S.; Baltrusaitis, J.; Cuadra-Rodriguez, L. A.; Collins, D. B.; Ruppel, M. J.; Bertram, T. H.; Prather, K. A.; Grassian, V. H. Inside versus outside: Ion redistribution in nitric acid reacted sea spray aerosol particles as determined by single particle analysis. *J. Am. Chem. Soc.* **2013**, *135* (39), 14528−14531.
(36) Sultana, C. M.; Cornwell, G. C.; Rodriguez, P.; Prather, K. A. FATES: a flexible analysis toolkit for the exploration of single-particle mass spectrometer data. *Atmos. Meas. Tech.* **2017**, *10* (4), 1323−1334.
(37) Ault, A. P.; Williams, C. R.; White, A. B.; Neiman, P. J.; Creamean, J. M.; Gaston, C. J.; Ralph, F. M.; Prather, K. A., Detection of Asian dust in California orographic precipitation. *J. Geophys. Res.* **2011**, *116*, (D16). DOI: 10.1029/2010JD015351
(38) Creamean, J. M.; Suski, K. J.; Rosenfeld, D.; Cazorla, A.; DeMott, P. J.; Sullivan, R. C.; White, A. B.; Ralph, F. M.; Minnis, P.; Comstock, J. M. Dust and biological aerosols from the Sahara and Asia influence precipitation in the western US. *Science* **2013**, *339* (6127), 1572−1578.
(39) Gaston, C. J.; Quinn, P. K.; Bates, T. S.; Gilman, J. B.; Bon, D. M.; Kuster, W. C.; Prather, K. A. The impact of shipping, agricultural, and urban emissions on single particle chemistry observed aboard the R/V Atlantis during CalNex. *J. Geophys. Res., [Atmos.]* **2013**, *118* (10), 5003−5017.
(40) Sullivan, R. C.; Guazzotti, S. A.; Sodeman, D. A.; Prather, K. A. Direct observations of the atmospheric processing of Asian mineral dust. *Atmos. Chem. Phys.* **2007**, *7* (5), 1213−1236.
(41) Bhave, P. V.; Allen, J. O.; Morrical, B. D.; Fergenson, D. P.; Cass, G. R.; Prather, K. A. A Field-Based Approach for Determining ATOFMS Instrument Sensitivities to Ammonium and Nitrate. *Environ. Sci. Technol.* **2002**, *36* (22), 4868−4879.
(42) Gross, D. S.; Gälli, M. E.; Silva, P. J.; Prather, K. A. Relative Sensitivity Factors for Alkali Metal and Ammonium Cations in Single-Particle Aerosol Time-of-Flight Mass Spectra. *Anal. Chem.* **2000**, *72* (2), 416−422.
(43) Spencer, M. T.; Holecek, J. C.; Corrigan, C. E.; Ramanathan, V.; Prather, K. A., Size-resolved chemical composition of aerosol

https://dx.doi.org/10.1021/acs.est.0c06067
Environ. Sci. Technol. XXXX, XXX, XXX−XXX

particles during a monsoonal transition period over the Indian Ocean. *J. Geophys. Res.* **2008**, *113*, (D16). DOI: 10.1029/2007JD008657
(44) Wenzel, R. J.; Liu, D.-Y.; Edgerton, E. S.; Prather, K. A., Aerosol time-of-flight mass spectrometry during the Atlanta Supersite Experiment: 2. Scaling procedures. *J. Geophys. Res.* **2003**, *108*, (D7). DOI: 10.1029/2001JD001563
(45) Thornton, J. A.; Abbatt, J. P. D. N_2O_5 Reaction on Submicron Sea Salt Aerosol: Kinetics, Products, and the Effect of Surface Active Organics. *J. Phys. Chem. A* **2005**, *109* (44), 10004−10012.
(46) Osthoff, H. D.; Roberts, J. M.; Ravishankara, A. R.; Williams, E. J.; Lerner, B. M.; Sommariva, R.; Bates, T. S.; Coffman, D.; Quinn, P. K.; Dibb, J. E.; Stark, H.; Burkholder, J. B.; Talukdar, R. K.; Meagher, J.; Fehsenfeld, F. C.; Brown, S. S. High levels of nitryl chloride in the polluted subtropical marine boundary layer. *Nat. Geosci.* **2008**, *1* (5), 324−328.
(47) Freney, E.; Martin, S.; Buseck, P. Deliquescence and Efflorescence of Potassium Salts Relevant to Biomass-Burning Aerosol Particles. *Aerosol Sci. Technol.* **2009**, *43*, 799−807.
(48) Gupta, D.; Eom, H. J.; Cho, H. R.; Ro, C. U. Hygroscopic behavior of NaCl−$MgCl_2$ mixture particles as nascent sea-spray aerosol surrogates and observation of efflorescence during humidification. *Atmos. Chem. Phys.* **2015**, *15* (19), 11273−11290.
(49) Gough, R. V.; Wong, J.; Dickson, J. L.; Levy, J. S.; Head, J. W.; Marchant, D. R.; Tolbert, M. A. Brine formation via deliquescence by salts found near Don Juan Pond, Antarctica: Laboratory experiments and field observational results. *Earth Planet. Sci. Lett.* **2017**, *476*, 189−198.
(50) Ordóñez, S.; Moral, S. S.; Cura, M. D. L. A. G. D.; Badiola, E. R.; Renaut, R. W.; Last, W. M., Precipitation of Salts from Mg^{2+}-(Na^{+})-So_4^{2-}-Cl− Playa−Lake Brines: The Endorheic Saline Ponds of La Mancha, Central Spain. In *Sedimentology and Geochemistry of Modern and Ancient Saline Lakes Models*; SEPM Society for Sedimentary Geology, 1994; Vol. *50*, p 0.
(51) Pakzad, H. R.; Ajalloeian, R. Geochemistry of the Gavkhoni Playa Lake Brine. *Carbonates Evaporites* **2004**, *19* (1), 67−74.
(52) McNeill, V. F.; Patterson, J.; Wolfe, G. M.; Thornton, J. A. The effect of varying levels of surfactant on the reactive uptake of N_2O_5 to aqueous aerosol. *Atmos. Chem. Phys.* **2006**, *6* (6), 1635−1644.
(53) Xia, M.; Wang, W.; Wang, Z.; Gao, J.; Li, H.; Liang, Y.; Yu, C.; Zhang, Y.; Wang, P.; Zhang, Y.; Bi, F.; Cheng, X.; Tao, W. Heterogeneous Uptake of N_2O_5 in Sand Dust and Urban Aerosols Observed during the Dry Season in Beijing. *Atmosphere* **2019**, *10*, 204.
(54) Tang, M. J.; Schuster, G.; Crowley, J. N. Heterogeneous reaction of N_2O_5 with Illite and Arizona test dust particles. *Atmos. Chem. Phys.* **2014**, *14* (1), 245−254.
(55) Messaoudi, S.; Béjaoui, B.; Akrout, F.; Hassen, M.; Sammari, C. Exploration of the Reactivity of N_2O_5 with two $Si(OH)_4$ Monomers using Electronic Structure Methods. *Int. J. Quantum Chem.* **2013**, *113*, 1633−1640.
(56) Seisel, S.; Börensen, C.; Vogt, R.; Zellner, R. Kinetics and mechanism of the uptake of N_2O_5 on mineral dust at 298 K. *Atmos. Chem. Phys.* **2005**, *5* (12), 3423−3432.
(57) Dall'Osto, M.; Harrison, R. M.; Beddows, D. C. S.; Freney, E. J.; Heal, M. R.; Donovan, R. J. Single-Particle Detection Efficiencies of Aerosol Time-of-Flight Mass Spectrometry during the North Atlantic Marine Boundary Layer Experiment. *Environ. Sci. Technol.* **2006**, *40* (16), 5029−5035.
(58) Silva, P. J.; Liu, D.-Y.; Noble, C. A.; Prather, K. A. Size and Chemical Characterization of Individual Particles Resulting from Biomass Burning of Local Southern California Species. *Environ. Sci. Technol.* **1999**, *33* (18), 3068−3076.
(59) Fenter, F. F.; Caloz, F.; Rossi, M. J. Heterogeneous Kinetics of N_2O_5 Uptake on Salt, with a Systematic Study of the Role of Surface Presentation (for N_2O_5 and HNO_3). *J. Phys. Chem.* **1996**, *100* (3), 1008−1019.
(60) Gaston, C. J.; Thornton, J. A.; Ng, N. L. Reactive uptake of N_2O_5 to internally mixed inorganic and organic particles: the role of organic carbon oxidation state and inferred organic phase separations. *Atmos. Chem. Phys.* **2014**, *14* (11), 5693−5707.
(61) Ryder, O. S.; Campbell, N. R.; Morris, H.; Forestieri, S.; Ruppel, M. J.; Cappa, C.; Tivanski, A.; Prather, K.; Bertram, T. H. Role of Organic Coatings in Regulating N_2O_5 Reactive Uptake to Sea Spray Aerosol. *J. Phys. Chem. A* **2015**, *119* (48), 11683−11692.
(62) Murphy, D. M.; Cziczo, D. J.; Froyd, K. D.; Hudson, P. K.; Matthew, B. M.; Middlebrook, A. M.; Peltier, R. E.; Sullivan, A.; Thomson, D. S.; Weber, R. J., Single-particle mass spectrometry of tropospheric aerosol particles. *J. Geophys. Res.* **2006**, *111*, (D23S32). DOI: 10.1029/2006JD007340
(63) Sarwar, G.; Simon, H.; Xing, J.; Mathur, R. Importance of tropospheric $ClNO_2$ chemistry across the Northern Hemisphere. *Geophys. Res. Lett.* **2014**, *41* (11), 4050−4058.
(64) Tham, Y. J.; Wang, Z.; Li, Q.; Wang, W.; Wang, X.; Lu, K.; Ma, N.; Yan, C.; Kecorius, S.; Wiedensohler, A.; Zhang, Y.; Wang, T. Heterogeneous N_2O_5 uptake coefficient and production yield of $ClNO_2$ in polluted northern China: roles of aerosol water content and chemical composition. *Atmos. Chem. Phys.* **2018**, *18* (17), 13155−13171.
(65) McDuffie, E. E.; Fibiger, D. L.; Dubé, W. P.; Lopez-Hilfiker, F.; Lee, B. H.; Thornton, J. A.; Shah, V.; Jaeglé, L.; Guo, H.; Weber, R. J.; Reeves, M. J.; Weinheimer, A. J.; Schroder, J. C.; Campuzano-Jost, P.; Jimenez, J. L.; Dibb, J. E.; Veres, P.; Ebben, C.; Sparks, T. L.; Wooldridge, P. J.; Cohen, R. C.; Hornbrook, R. S.; Apel, E. C.; Campos, T.; Hall, S. R.; Ullmann, K.; Brown, S. S. Heterogeneous N_2O_5 Uptake During Winter: Aircraft Measurements During the 2015 WINTER Campaign and Critical Evaluation of Current Parameterizations. *J. Geophys. Res., [Atmos.]* **2018**, *123* (8), 4345−4372.
(66) Staudt, S.; Gord, J. R.; Karimova, N. V.; McDuffie, E. E.; Brown, S. S.; Gerber, R. B.; Nathanson, G. M.; Bertram, T. H. Sulfate and Carboxylate Suppress the Formation of $ClNO_2$ at Atmospheric Interfaces. *ACS Earth Space Chem.* **2019**, *3* (9), 1987−1997.
(67) Goodman, M. M.; Carling, G. T.; Fernandez, D. P.; Rey, K. A.; Hale, C. A.; Bickmore, B. R.; Nelson, S. T.; Munroe, J. S. Trace element chemistry of atmospheric deposition along the Wasatch Front (Utah, USA) reflects regional playa dust and local urban aerosols. *Chem. Geol.* **2019**, *530*, 119317.

https://dx.doi.org/10.1021/acs.est.0c06067
Environ. Sci. Technol. XXXX, XXX, XXX−XXX